Computer Physics Communications 307 (2025) 109394

Contents lists available at ScienceDirect

Computer Physics Communications

journal homepage: www.elsevier.com/locate/cpc

Computational Physics

SU2-COOL: Open-source framework for non-ideal compressible fluid dynamics ☆

Peng Yan [a], Giulio Gori [a], Marta Zocca [b], Alberto Guardone [a,b,*]

[a] Politecnico di Milano, Department of Aerospace Science and Technology, Via La Masa, 34, Milano, 20156, Italy
[b] Lappeenranta-Lahti University of Technology, LES, Fluid Dynamics, Yliopistonkatu 34, Lappeenranta, 53850, Finland

ARTICLE INFO

Keywords:
Open-source
Non-ideal compressible fluid dynamics NICFD
SU2
CoolProp
Non-monotone Mach number
Non-classical rarefaction shock

ABSTRACT

We present a fully open-source framework for the numerical simulation of Non-Ideal Compressible Fluid Dynamics (NICFD). The open-source Computational Fluid Dynamics suite SU2 is coupled to the open-source thermophysical library CoolProp, which includes state-of-the-art thermodynamic models of numerous pure fluids and mixtures relevant to applications. Accurate thermodynamic models are needed due to non-ideal operating conditions in which the fluid thermodynamics cannot be described by the simple ideal-gas law ($Pv = RT$). The coupling interface implements new C++ classes, which allow the automatic exchange of information between SU2 and CoolProp, and it is made directly available as an additional module integrated into the open-source SU2 suite. To assess the performance of the NICFD simulation framework, we present three test cases: a nozzle flow exhibiting non-ideal thermodynamics effects, a nozzle flow with non-monotone Mach number variation, a representative non-ideal gasdynamics effect, and a non-classical rarefaction oblique shock over a wedge. Results are verified against available experiment data and solutions obtained with different implementations of non-ideal thermodynamics in SU2. Performance of the new framework is assessed on user-friendliness, scalability, solution accuracy, and computational efficiency.

1. Introduction

The thermodynamics and gasdynamics of fluid flows in thermodynamic conditions near the liquid-vapor saturation curve and critical point, or the supercritical region, differs significantly from the one predicted under the ideal, dilute gas assumption, namely, $Pv = RT$, with P pressure, v specific volume, R gas constant, and T temperature. Compared to ideal, dilute-gas conditions, non-ideal thermodynamics results in quantitatively different flow evolution. Moreover, non-ideal gas dynamics effects might occur, which change the qualitative behavior of the flow. Non-ideal gasdynamic effects include non-monotone Mach evolution along isentropic expansions, Mach-increasing oblique shock waves or rarefaction and mixed shock waves. The branch of fluid mechanics describing the quantitative and qualitative effects on the flow field due to the non-ideal thermodynamics properties is termed Non-Ideal Compressible Fluids Dynamics (NICFD). A review of NICFD fundamentals and applications is given in [1]. NICFD is relevant to numerous, heterogeneous industrial applications, such as Organic Rankine cycle [2], heat pumps [3], supercritical CO_2 power systems [4], Rapid Expansion of Supercritical Solution [5].

The compressibility factor

$$Z = \frac{Pv}{RT}, \tag{1}$$

quantifies the deviation of the thermodynamic behavior of the flow from ideality. A unit compressibility factor $Z \equiv 1$ indicates ideal conditions ($Pv \equiv RT$), whereas $Z \neq 1$ suggests that the thermodynamics no longer abide by the ideal gas law. Quantitatively, non-ideal effects become more relevant with Z departing from unity. In addition, the dimensionless fundamental derivative of gasdynamics Γ [6]

$$\Gamma = 1 + \frac{c}{v}\left(\frac{\partial c}{\partial P}\right)_s, \tag{2}$$

with c speed of sound, v specific volume and s entropy, accounts for the caloric non-ideality, and its value determines the possibility of the occurrence of non-ideal gasdynamics effects. In particular, non-ideal

☆ The review of this paper was arranged by Prof. Peter Vincent.

* Corresponding author at: Politecnico di Milano, Department of Aerospace Science and Technology, Via La Masa, 34, Milano, 20156, Italy.
E-mail addresses: peng.yan@polimi.it (P. Yan), giulio.gori@polimi.it (G. Gori), marta.zocca@lut.fi (M. Zocca), alberto.guardone@polimi.it (A. Guardone).

https://doi.org/10.1016/j.cpc.2024.109394
Received 8 March 2024; Received in revised form 9 July 2024; Accepted 7 October 2024
Available online 28 October 2024

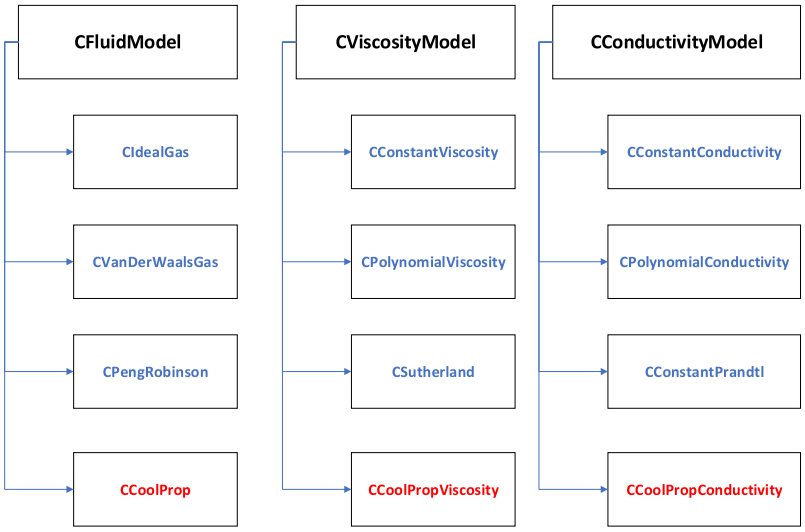

Fig. 1. Classes related to thermophysical models in SU2. Parent classes, child classes, new child classes as interface between SU2 and CoolProp.

gasdynamics effects are admissible only if $\Gamma < 1$. Note that the parameter Γ is constant for an ideal gas with constant specific heats.

Experimental activities are underway to characterize both thermodynamics and gasdynamics non-ideal phenomena. Unfortunately, data concerning highly non-ideal flow are still scarce due to the inherent difficulty of achieving the extreme operating conditions required to attain a non-ideal state of the fluid, as reviewed in Ref. [1].

Computational Fluid Dynamics (CFD) is a valuable tool for investigating NICFD flows and designing machinery operating in the NICFD regime. In NICFD conditions, the properties of the fluid depart significantly from those predicted using the ideal gas law, thus requiring the use of complex thermodynamic models in CFD codes. Several CFD solvers, both open-source [7–9] and commercial [10] have been extended to accommodate the simulation of non-ideal flow applications. In SU2, the integrated thermodynamic library embeds non-ideal fluid models such as the van der Waals model, the improved Peng-Robinson Stryjek-Vera model (PR), and boundary conditions tailored to NICFD flows [7]. The accuracy of the SU2 toolkit for NICFD applications was assessed first in Refs. [11,12].

Thermodynamic libraries such as e.g. RefProp [13], FluidProp [14], and the open-source CoolProp [15] provide a highly accurate description of thermodynamics and transport properties in NICFD flows. RefProp and FluidProp are not released open-source.

This paper aims to present a fully open-source framework for the numerical simulation of NICFD flows. The open-source toolkit SU2 suite is coupled to the open-source thermophysical library CoolProp [15]. CoolProp is a C++ library implementing pure and pseudo-pure state-of-the-art fluid models, including models for evaluating transport properties for more than 120 substances. Thermodynamic properties are evaluated using a high-accuracy multiparameter equation of state based on Helmholtz energy formulations (HEOS). In computationally demanding applications, the thermodynamic state of the fluid may be retrieved through efficient tabular interpolation. A CoolProp wrapper is already available for the OpenFOAM CFD solver [9].

This paper is organized as follows. In Sec. 2, the coupling of SU2 and CoolProp is described in detail. In Sec. 3, verification and validation results are presented. Assessment of SU2-COOL performance is discussed in Sec. 4. Conclusions are drawn in Sec. 5.

2. Code framework and design

2.1. SU2 thermophysical classes

SU2 is an open source computational suite for solving partial differential equation (PDE) problems on unstructured meshes. The core tools of the SU2 suite are C++ executables under object-oriented framework. Modules in SU2 are designed in a way leveraging class inheritance and polymorphism. In these modules, header `.hpp` and source files `.cpp` of classes are stored in `include` and `src` subfolders separately. More details of code structure can be found in [16].

In SU2, the parent class for defining the thermodynamics model is `CFluidModel` where the protected members include pressure, temperature, density, static energy, speed of sound, etc. Its child class include `CIdealGas` providing polytropic ideal gas model (PIG) and `CVanDerWaalsGas`, `CPengRobinson` storing non-ideal polytropic van der waals (PVdW) and Peng-Robinson (PR) models. Similarly, the parent classes `CViscosityModel`, `CConductivityModel` store the value of viscosity and conductivity, and both of them have related child classes.

The relation between these classes is illustrated in Fig. 1.

2.2. CoolProp library

CoolProp is an open source thermophysical library with C++ codes as its cores. It implements the state-of-the-art HEOS for modeling fluid thermodynamics and transport properties. All interested thermodynamic parameters can be computed from the partial derivatives of the Helmholtz energy. CoolProp has two interfaces: high level and low level. High level interface is more simple to use while low level interface is much faster without string comparison and parsing. Hence, low level in C++ is used in this work.

At the C++ level, the code is based on the use of a base class `AbstractState`. The property backends (e.g., HEOS) are required to implement a protocol defined by the base class. Once the backend and fluid name are given, thermophysical properties can be evaluated from any two independent variables. An example of computing density from pressure/temperature with HEOS backend for water is:

```
1 fluid_entity = std::unique_ptr<CoolProp::AbstractState>(CoolProp
      ::AbstractState::factory("HEOS", water));
2 fluid_entity->update(CoolProp::PT_INPUTS, P, T);
3 rho = fluid_entity->rhomass();
```

2.3. Interface

The coupling interface linking the open-source thermophysical library CoolProp to the open-source CFD suite SU2 is based on the implementation of the following three C++ classes:

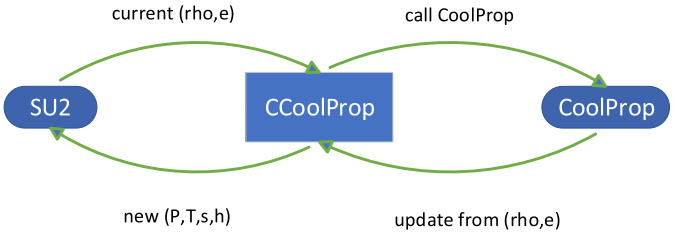

Fig. 2. Flowchart of data exchange between SU2 and CoolProp via c++ class `CCoolProp`.

- `CCoolProp`. General class for computing thermodynamic quantities (pressure, temperature, entropy, enthalpy) from the conservative variables density, momentum and total energy density used in the CFD solver.
- `CCoolPropViscosity`. Class for transport property viscosity.
- `CCoolPropConductivity`. Class for transport property thermal conductivity.

Modification of other codes in SU2 is trivial and neglected here.

Fig. 2 conceptualizes the computation of the fluid thermodynamic state between SU2 and the CoolProp thermodynamic library. First the internal energy e is computed from the conservative variables density ρ, momentum m and total energy per unit volume E_t as $e = \frac{E_t}{\rho} - \frac{1}{2}(\frac{m}{\rho})^2$. At each iteration of the CFD solver, the (ρ, e) *tuple* (two independent thermodynamic variables specifying the current thermodynamic state at a grid node) is passed to the `CCoolProp` class, which then calls the required thermodynamic routines within the CoolProp library to compute all thermodynamics quantities. Thermodynamic quantities are then passed back to SU2 through the class `CCoolProp`, and the CFD solver proceeds to the next solution step. An analogous implementation is used for evaluating transport properties via the `CCoolPropViscosity` and the `CCoolPropConductivity` classes. These are tasked to compute the value of the fluid viscosity and thermal conductivity, respectively.

Notice that in CoolProp, viscosity and conductivity model are not available for some fluids. Hence a private member `FluidNameList` is defined in class `CCoolPropViscosity, CCoolPropConductivity`. Only fluids listed in `FluidNameList` can update transport properties using CoolProp library.

2.4. Compilation and use

The SU2-COOL framework is freely available from the `master` branch in the `SU2` GitHub repository [17]. An automated procedure allows to couple SU2 to the CoolProp library by activating the configuration flag

`-Denable-coolprop=true` during the installation.

The fully command to compile SU2 and CoolProp is:

```
$./meson.py build -Denable-coolprop=true --prefix=
```

To use SU2-COOL, only one input is required in the config file: fluid name, like:

```
FLUID_NAME = Water
```

3. Verification and validation

Three reference test cases are now considered to verify the SU2-COOLProp framework. The first case in section 3.1 is a nozzle flow expansion in non-ideal conditions, where only non-ideal thermodynamic effects are observed. Simulations are validated against experimental results from the TROVA facility of Politecnico di Milano [18]. In section 3.2, the second test case addresses non-ideal gasdynamics effects. In particular, the non-monotone Mach number evolution in a gasdynamic nozzle is studied. Finally, the third case in section 3.3 reports on numerical simulations of a non-classical rarefaction shock wave over a wedge.

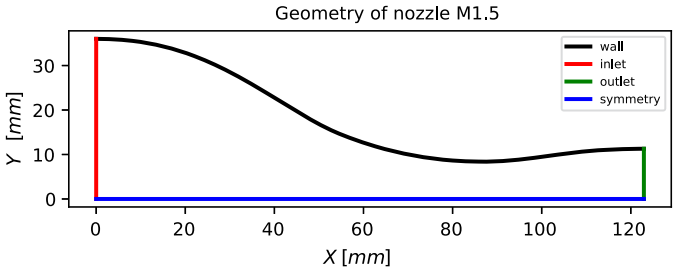

Fig. 3. Computational domain and boundary conditions. The total temperature T_t and total pressure P_t are imposed at the inlet. The ambient pressure P_a is set at the outlet.

Table 1
Fluid working conditions for the ideal gas and the non-ideal regimes.

Case name	Fluid	P_t [bar]	T_t [C°]	Z_t	Γ_t	P_a [bar]
Ideal	N_2	1.00	26.85	0.99	1.20	0.4
Non-ideal	MDM	9.04	268.98	0.65	0.47	2.0

3.1. Non-ideal thermodynamics effects in nozzle flows

We consider diatomic nitrogen N_2 and the molecular complex siloxane fluid MDM (octamethyltrisiloxane, $C_8H_{24}Si_3O_2$), expanding to supersonic speed in a planar converging-diverging nozzle. The test case geometry from [18] is available in the tutorial *Non-ideal compressible flow in a supersonic nozzle* in the SU2 repository, see [17]. The computational domain corresponds to the nozzle internal channel, depicted in Fig. 3.

Two working conditions, representative of an ideal and a non-ideal regime, are considered and summarized in Table 1, where the subscript t and a refer to the total and ambient conditions, respectively.

Experimental data for this test case, together with details concerning the setup of the test rig, are reported in [18].

3.1.1. Ideal gas conditions

We start by considering diatomic nitrogen N_2 in ideal, dilute-gas conditions, see Table 1. The flow exhibits an ideal behavior since $Z_t \sim 1$ and $\Gamma_t > 1$. The goal of the present comparison is to verify that the solution obtained with the SU2-COOL toolkit using the complex thermodynamic models reduces to the one computed by SU2 using the ideal gas law in dilute conditions, where the two models predict the same properties.

The `EULER` model is used to simulate the test case under the assumption of inviscid compressible flow according to the boundary layer approximation. Moreover, the geometry is two-dimensional and the flow is assumed to be steady. Since the flow is inviscid, the boundary condition at the nozzle wall is a slip, non-penetrating condition. The thermodynamics model is the HEOS provided by the CoolProp library. The numerical flux is a Roe scheme with a Monotonic Upstream-centered Scheme for Conservation Laws (MUSCL) approach. Simulations are evolved over pseudo time until a steady condition is achieved. The convergence indicator is the root mean square of the density residual. Convergence is achieved if the magnitude of the indicator is lowered by a factor of 9 orders of magnitude with respect to the initial residual. The maximum number of iterations is set to 10 000. The mesh of unstructured triangular elements is generated using the open-source software Gmsh [19].

In Fig. 4, we compare numerical predictions concerning the static-to-total pressure ratio P/P_t and Mach number distribution along the nozzle centerline for the three different considered mesh, made of 5 000, 12 000 and 22 000 elements, respectively. The three plots for the pressure ratio and the Mach number on the nozzle centerline shown in Fig. 4a, 4b are

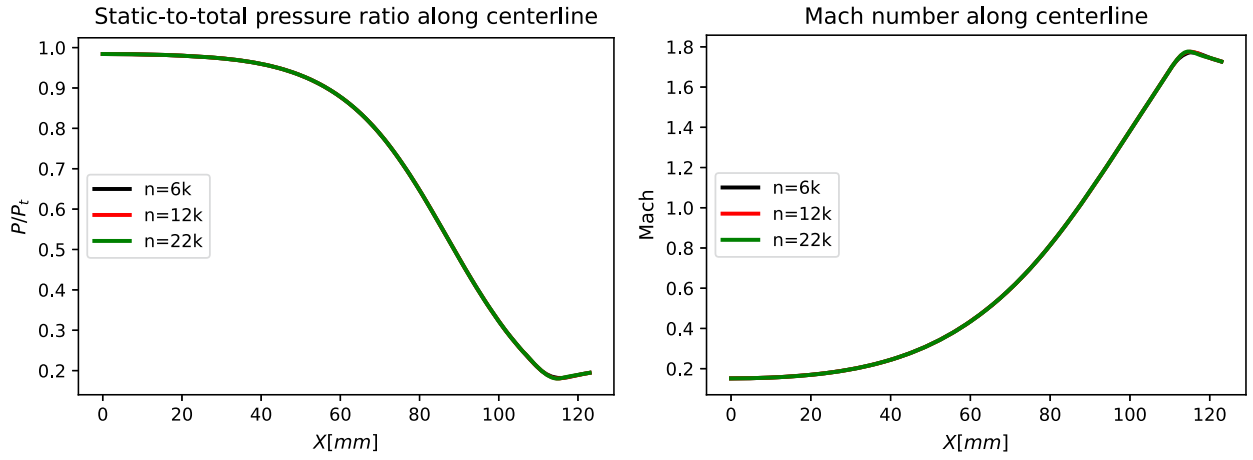

(a) Static-to-total pressure ratio P/P_t (b) Mach number

Fig. 4. Inviscid ideal case. Flow variables along the centerline of the nozzle for different grids with increasing number of elements n.

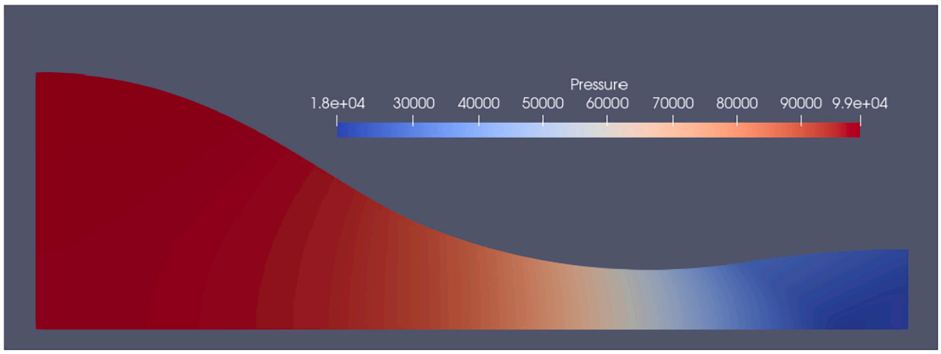

Fig. 5. Inviscid ideal gas. Predicted pressure field (grid $n = 22\,000$).

perfectly overlapping, suggesting the achievement of a grid-independent solution. The grid with 22 000 cells is used for the following analyses. The density residual converges in about 650 iterations for the grid with 22 000 cells.

The predicted pressure field is shown in Fig. 5. The field is continuous, and gradients appear smooth, as expected since the nozzle operates at design conditions.

Fig. 6 compares the profile of the static-to-total pressure ratio P/P_t extracted along the nozzle centerline against the same quantity computed using the SU2 embedded polytropic (constant specific heats) ideal gas model (PIG). The PIG curve (black line) is superimposed on the CoolProp (red line), indicating that in ideal conditions, the solution predicted by the proposed framework reduces to the ideal one computed by the standard SU2 solver. To better highlight this verification result, we also report the maximum difference of the pressure ratio Δ_{P/P_t} between the HEOS and the polytropic ideal-gas model, defined as

$$\Delta_{P/P_t} = 100 \cdot \left| 1 - \frac{(P/P_t)_{\text{HEOS}}}{(P/P_t)_{\text{PIG}}} \right| \tag{3}$$

From Fig. 6, the maximum Δ_{P/P_t} is around 0.25%, which is negligible.

Viscous-flow simulations are now considered using the Menter's Shear Stress Transport (SST) closure [20]. Transport properties are computed using the CoolProp library. Adiabatic non-slip boundary conditions are set at the wall of the nozzle.

The hybrid grid in Fig. 7 is generated using Gmsh. A structured, boundary-layer grid is used close to the nozzle wall; triangular elements are used in the outer, inviscid flow. At the wall, the boundary layer grid is generated so to ensure that the height of the first layer lies approximately in the region $y^+ \approx 1$. The grid convergence study in Fig. 8 shows that a grid with 19 000 elements guarantees grid independence of the solution. The density residual decreases by 9 orders of magnitudes at the

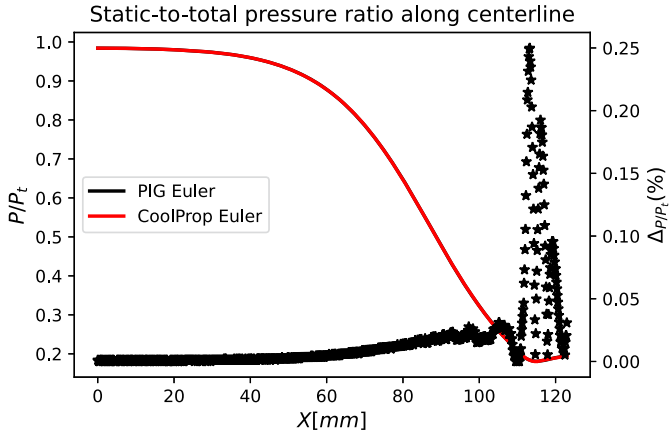

Fig. 6. Inviscid ideal gas. Comparison of the distribution of P/P_t along the centerline for the PIG and CoolProp models in ideal conditions and relative difference (black stars) from the HEOS and the ideal gas model. (For interpretation of the colors in the figure(s), the reader is referred to the web version of this article.)

maximum iteration number (10 000 iterations). The pressure along the nozzle centerline against the same quantity computed from SU2 with PIG is shown in Fig. 9, where the maximum Δ_{P/P_t} is around 0.16%.

3.1.2. Non-ideal conditions

To simulate the flow in the NICFD regime, we consider a molecularly complex fluid, namely, siloxane MDM ($C_8H_{24}O_2Si_3$), and assume the non-ideal working conditions summarized in Table 1. Constant viscosity and conductivity coefficients are assumed, consistently with the default

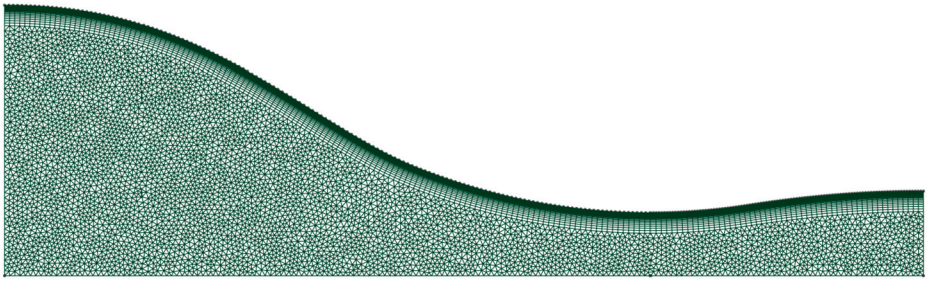

Fig. 7. Grid for the viscous case with 19 000 hybrid quadrilateral/triangle elements.

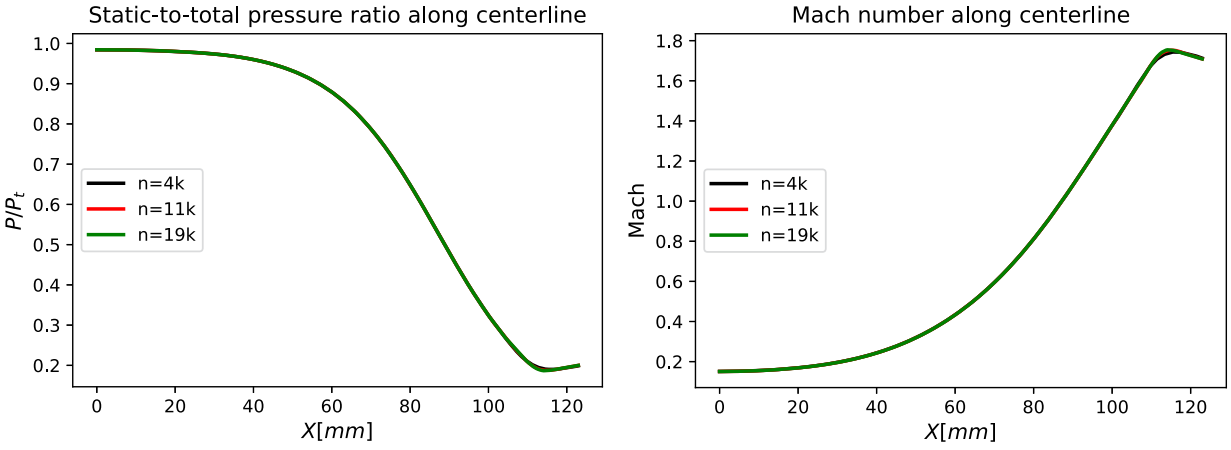

(a) Static-to-total pressure ratio P/P_t (b) Mach number

Fig. 8. Viscous ideal case. Flow variables along the centerline of the nozzle for different grids with increasing number of elements n.

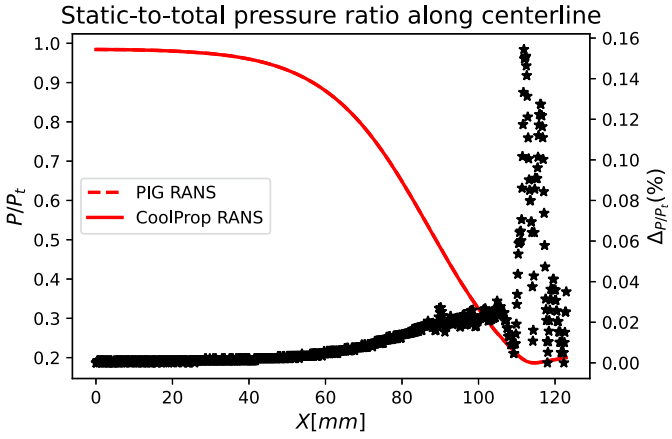

Fig. 9. Viscous dilute gas case. Comparison of the distribution of P/P_t along the centerline between PIG and CoolProp.

values provided by SU2. The HEOS thermodynamics model is provided by the CoolProp library.

The grid convergence study performed in the previous section is repeated here for the non-ideal case under both inviscid and viscous assumptions. Results are shown in Fig. 10a, 10b. Pressure profiles computed over different grids overlap, confirming grid independence. Convergence requires about 750 steps.

Fig. 11 reports the pressure field predicted by the CFD solution. Fig. 12 reports the comparisons of CFD computations using the SU2-COOL framework against results for different fluid models and methods. Results for the Peng-Robinson model (PR) model coded in SU2 and the FluidProp library coupled to SU2 are taken from Ref. [7,21]. For the supersonic portion only, we report predictions obtained using the method of characteristic for non-ideal fluids (NIMOC) [22]. Experimental data available from Ref. [18] are also reported for this test case. Note that experimental data are complemented by error bars with minimal amplitude, which are very small at the graph scale. The maximum relative difference Δ between experiment data and numerical results is smaller than 5%, which verifies the accuracy of CoolProp fluid model in the non-ideal regime.

3.2. Non-ideal gasdynamics effects in nozzle flows

An interesting non-ideal effect is the non-monotone variation of the Mach number along an isentropic expansion. From the quasi-one dimensional theory for steady, inviscid, adiabatic flow without body forces [23], the Mach number variation along an isentrope abides by

$$\frac{dM}{d\rho}(\rho; s, h^t) = \frac{M(\rho; s, h^t)}{\rho}\left(1 - \Gamma(s,\rho) - \frac{1}{M^2(\rho; s, h^t)}\right). \tag{4}$$

In the ideal gas regime, $\Gamma > 1$, and therefore the Mach number can only increase monotonically with decreasing density. However, in non-ideal conditions, Γ might be lower than one, thus opening the possibility of a nonmonotonic Mach number variation with decreasing density. We show this non-ideal gasdynamic effect in a two-dimensional steady, inviscid, and isentropic nozzle flow. The test conditions and the geometry are taken from Ref. [22]. The geometry of the nozzle is specifically designed to produce the desired non-ideal non-monotonic Mach number variation along the centerline. The mesh generated by Gmsh is fully unstructured with triangular elements.

For the present test case, we consider siloxane fluid MM ($C_6H_{18}OSi_2$). Operating conditions are summarized in Table 2.

The grid convergence study in Fig. 13 shows the Mach number value along the centerline for different grid resolutions. A region of non-monotonic Mach number variation is observed between $x \approx 0$ and $x \approx 5$, with $x = 0$ the nozzle throat, see Fig. 13. The density residual drops by 9 orders of magnitude after 800 iterations. The Mach number field predicted by our CFD framework is shown in Fig. 14.

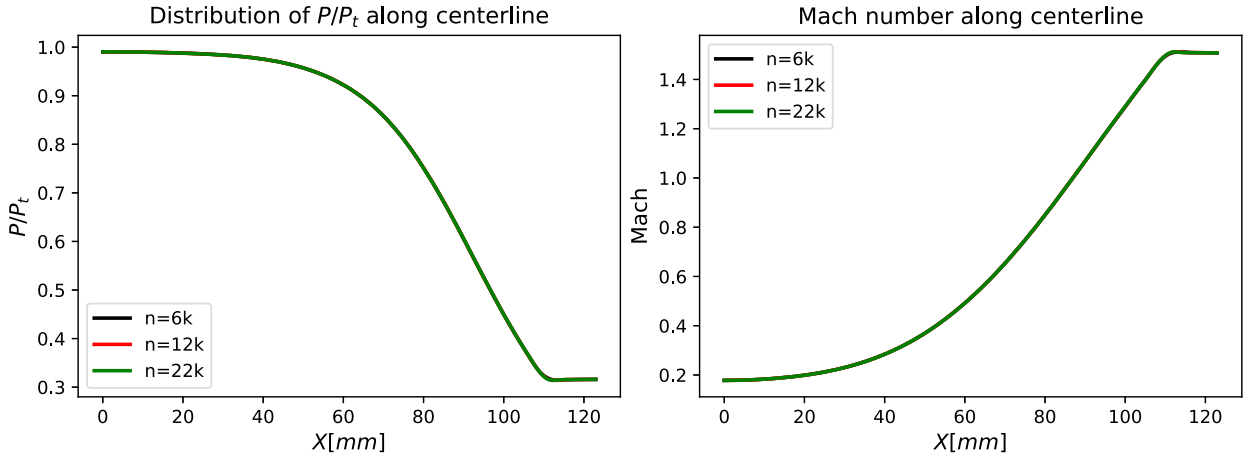

(a) Static-to-total pressure ratio P/P_t (b) Mach number

Fig. 10. Inviscid non-ideal case. Flow variables along the centerline of the nozzle for different grids with increasing number of elements n.

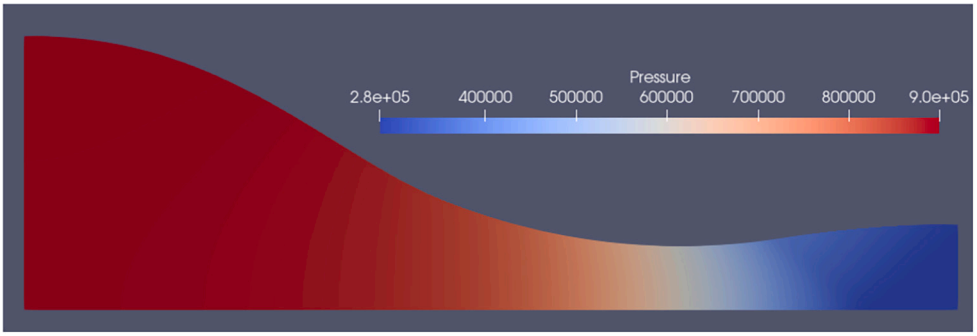

Fig. 11. Inviscid non-ideal case. Predicted pressure field (grid n = 22 000).

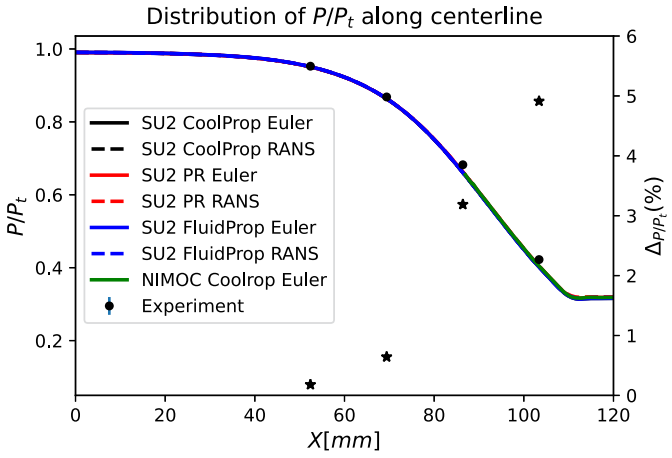

Fig. 12. Non-ideal case under the inviscid and viscous flow assumptions. Distribution of P/P_t along the centerline against experiments and different models and methods already available in the literature. The relative difference is also shown.

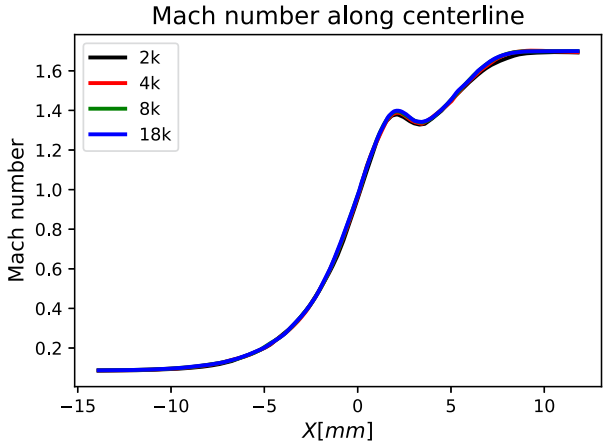

Fig. 13. Grid convergence study for the non-monotone Mach number test case.

Table 2
Working conditions for the non-monotone Mach number test case.

Fluid	P_t [bar]	T_t [C°]	Z_t	Γ_t	P_a [bar]
MM	29.5	265	0.29	4.03	4

The comparison of numerical prediction between the standard SU2 solver with the PR model, the NIMOC-CoolProp solver, and the present SU2-COOL framework are reported in Figs. 15(a-f), for the static pressure, the static temperature, the static density, the compressibility factor, the Mach number, and the derivative of the Mach number w.r.t. the density from the post-process results. From Fig. 15f, $dM/d\rho$ is negative except for $x \in [2, 3.5]$ mm, see Fig. 15e.

NIMOC-CoolProp and SU2-COOL deliver identical results, thus confirming the correctness of the implementation. As expected, the density computed by the PR model, and hence the compressibility factor and the Mach number derivatives, differs significantly from the one obtained by the more accurate HEOS model, a well-known limitation of cubic equations of state.

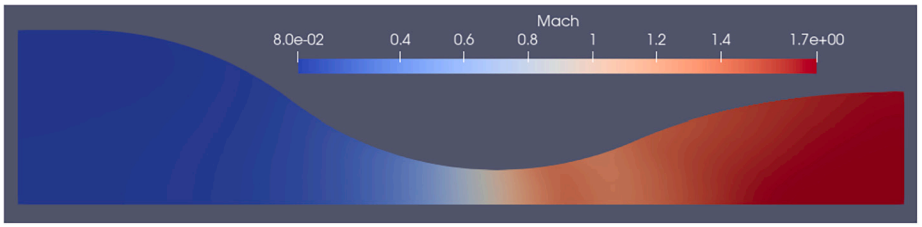

Fig. 14. Non-monotone Mach number test case. Predicted Mach number field (grid $n = 18\,000$).

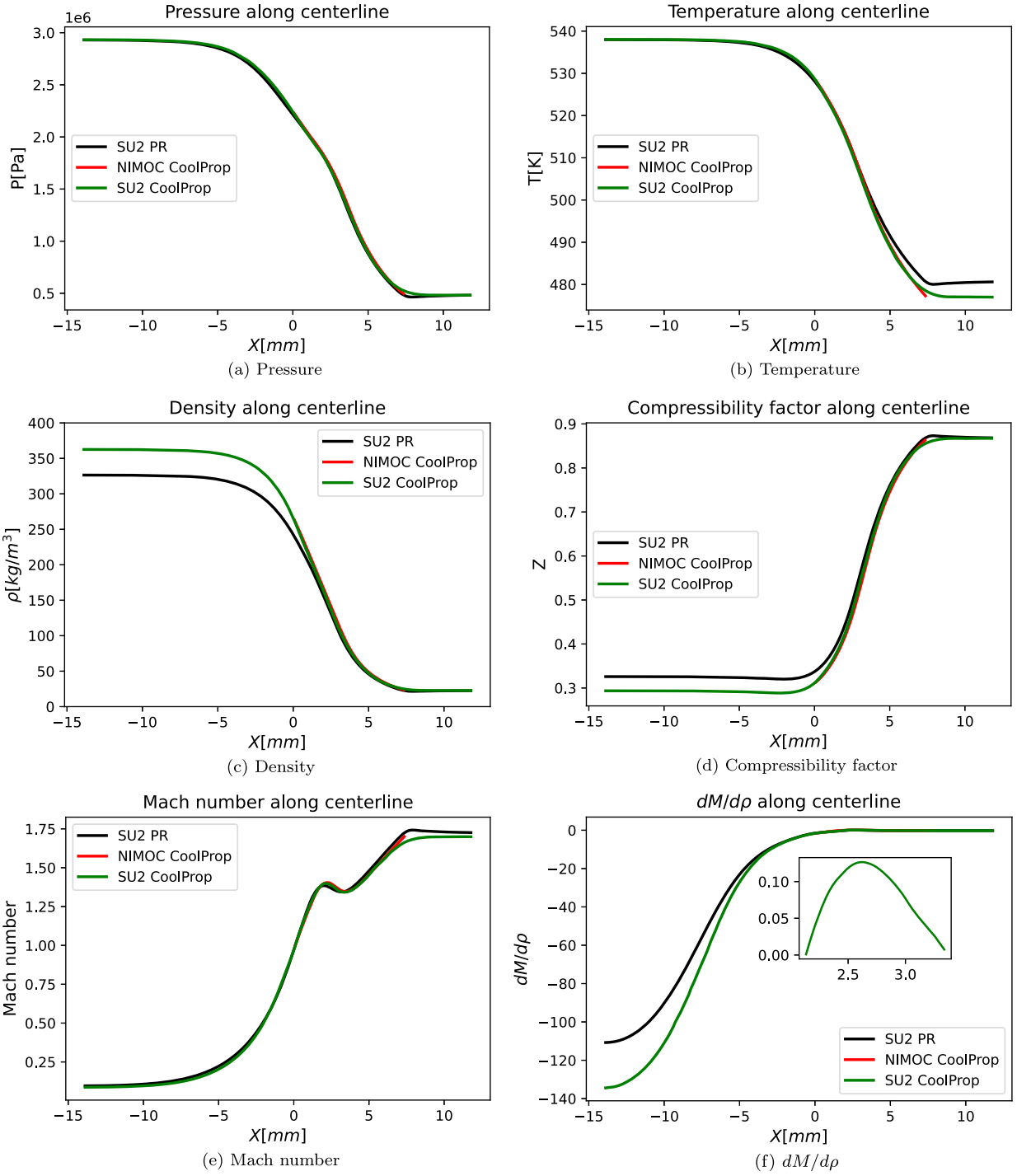

(a) Pressure (b) Temperature (c) Density (d) Compressibility factor (e) Mach number (f) $dM/d\rho$

Fig. 15. Non-monotone Mach number test case. Distribution of flow variables along the centerline. Comparison between results obtained with SU2 PR, SU2 CoolProp, NIMOC CoolProp.

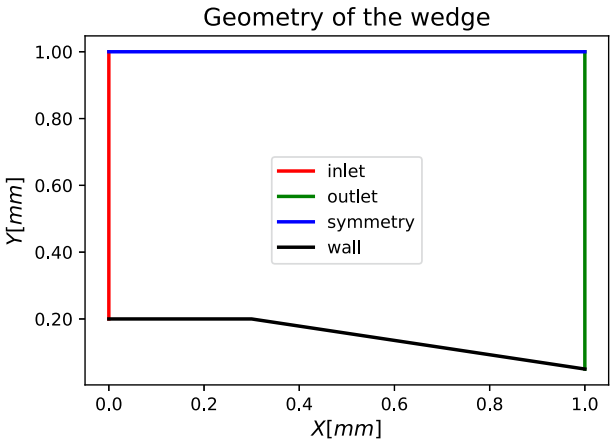

(a) Wedge with $\theta = 12.1^o$ deflection angle and boundary conditions.

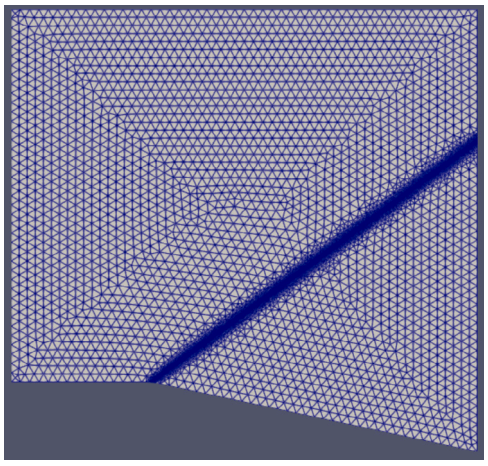

(b) Triangular grid with 140 000 elements.

Fig. 16. Geometry and computational mesh used in the computation of the non-classical shock wave case.

Table 3
Non-classical rarefaction shock wave. Pre-shock state (pressure, density, temperature reduced by fluid critical values, Z, Γ calculated using CoolProp).

Fluid	P_1	ρ_1	T_1	M_1	Z_1	Γ_1
MD_4M	0.99	0.80	0.99	1.70	0.33	0.33

Table 4
Shock angle (degree) obtained from theory and CFD.

Theory	36.506
CFD	36.607

Table 5
Non-classical rarefaction shock wave. Post-shock states were evaluated using different fluid models (density, pressure, and temperature reduced by fluid critical values).

Model	P_2	ρ_2	T_2	M_2	Z_2	Γ_2
PVdW	0.922	0.493	0.983	1.377	0.509	0.245
PR	0.889	0.518	0.988	1.409	0.533	0.147
CoolProp	0.887	0.522	0.991	1.307	0.458	0.007

3.3. Non-classical oblique shock wave

The third test case concerns a non-classical rarefaction shock wave over a wedge, which is physically admissible only if the shock crosses or it is embedded in the $\Gamma < 0$ region [6]. The computational domain is the same of Ref. [21] except the deflection angle is smaller, see in Fig. 16a. The fluid and working conditions ahead of the shock are listed in Table 3. Note that we identify the pre-shock state with subscript 1, whereas we employ subscript 2 for labeling the post-shock variables. The mesh with 140k elements is obtained with gradient-density mesh adaptation as described in Ref. [24], see Fig. 16b.

A grid convergence study is performed in terms of P/P_c, Mach number, ρ/ρ_c and Γ along $y = 0.3$ mm, shown in Fig. 17.

The considered grids are composed by 22k, 40k, 74k, and 140k elements. The curves associated to the n = 74k and n = 140k grids overlap. Residual of density decreases by orders of 3 and becomes constant after around 1000 steps.

The Mach number, reduced pressure and reduced density decrease rapidly around $X = 0.4$ mm, which indicates the existence of the rarefaction shock. The corresponding negative Γ can be found in Fig. 17d. The computed shock angle agrees with the theoretical prediction, see Table 4. The predicted pressure field is shown in Fig. 18.

Not surprisingly, the pressure field presents two homogeneous regions of uniform pressure separated by the oblique non-classical rarefaction shock. Across the shock, the static pressure drops about 10% of its upstream value. The post-shock states predicted numerically using the SU2-PVdW, SU2-PR, and our SU2-COOLProp framework are compared in Table 5. The results obtained with PVdW obviously differ from others. The difference of Z_2, Γ_2 from PR and CoolProp is large, 13%, 95% respectively.

4. Assessment of performance

In this section, the performance of the new framework SU2-COOL is assessed from different aspects.

4.1. User-friendliness

SU2-COOL is more user-friendly compared with SU2-PIG, SU2-PVdW and SU2-PR. The latter three required trivial inputs which are independent on thermodynamics states: specific heat ratio γ, gas constant R, acentric factor ω, critical pressure/temperature P_c, T_c of the given fluid from users. By comparison, the only input from user for SU2-COOL is the fluid name and trivial inputs are pre-stored in CoolProp library. For example, to switch PIG to CoolProp, an comparison of config file for defining fluid model of Nitrogen N_2 is shown:

```
# SU2-PIG
FLUID_MODEL = IDEAL_GAS
# SU2-COOL
FLUID_MODEL = COOLPROP
FLUID_NAME = Nitrogen
```

4.2. Scalability

To assess the scalability of SU2-COOL, the computational time is compared for the same simulation with increasing number of grid elements and increasing number of CPU cores for parallel computation. All three test cases in Sec. 3 are considered. Note that in first test case only inviscid non-ideal conditions are considered. For simplicity, we label the non-ideal thermodynamics nozzle as Nozzle A, non-ideal gasdynamics nozzle as Nozzle B and the non-classical oblique shock as NCSHOCK.

For each test case, only either number of grid elements or number of CPU cores is different while other numerical setup is same. All simulation run for 100 steps. Results are shown in Fig. 19. The time along y axis

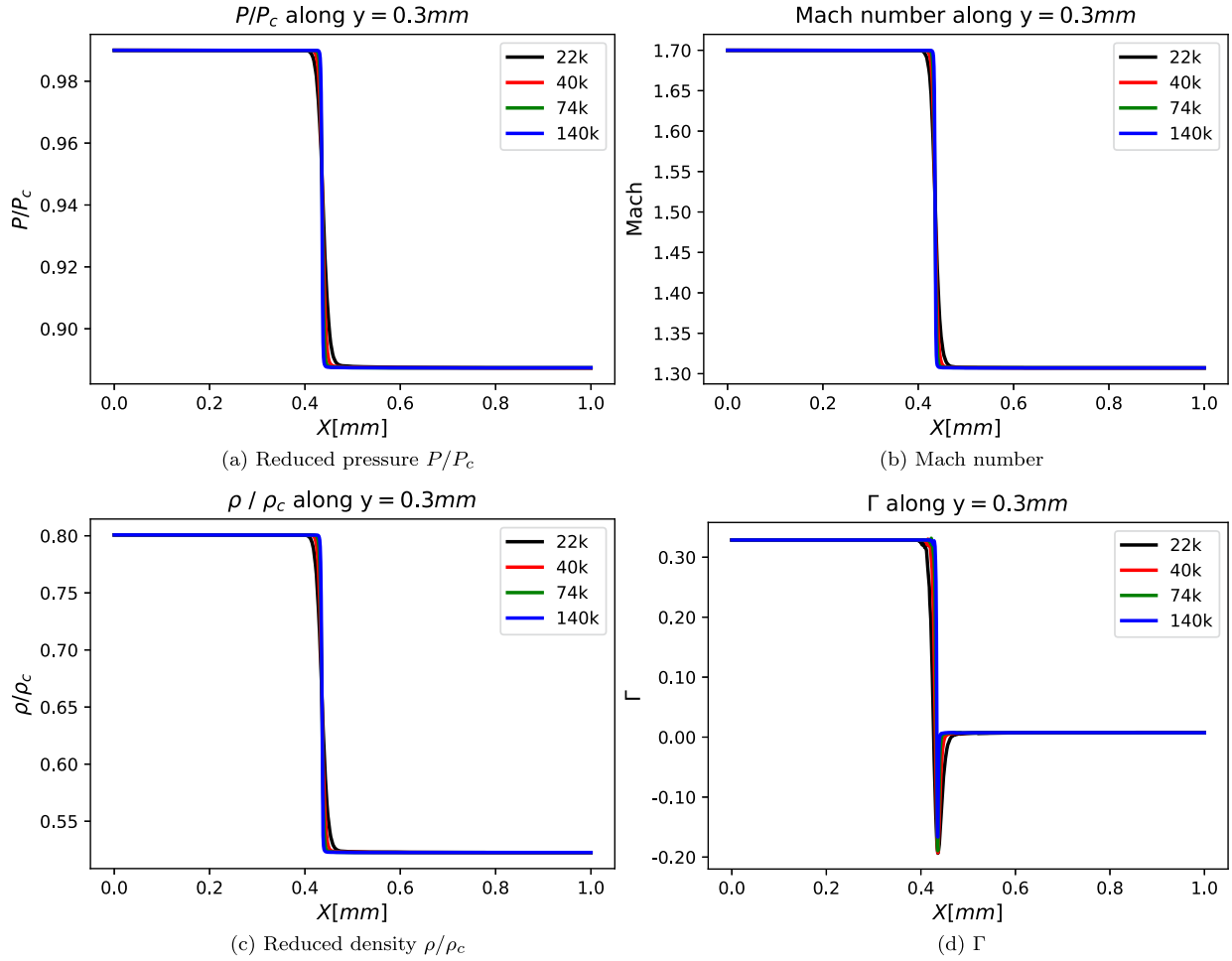

(a) Reduced pressure P/P_c (b) Mach number

(c) Reduced density ρ/ρ_c (d) Γ

Fig. 17. Non-classical rarefaction shock wave. Grid convergence study in terms of P/P_c, Mach number, ρ/ρ_c and Γ along $y = 0.3$ mm.

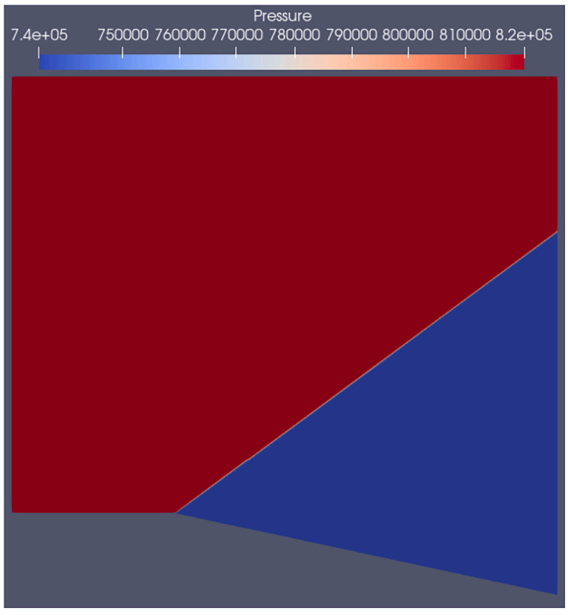

Fig. 18. Non-classical rarefaction shock wave. Predicted pressure field (n = 140k grid).

in Fig. 19a, 19b is normalized by the least time related to the coarsest grid or the most number of CPU cores, respectively. The computational time increases with the number of grid elements almost linearly, which indicates the computation time will not explode with increasing workloads. Besides, the computational time decreases with number of CPU cores approximately quadratically. Hence, we can expect the computational time will decrease dramatically with increasing number of CPU cores. Results in Fig. 19 show good scalability of SU2-COOL.

4.3. Solution accuracy

In Sec. 3, SU2-COOL has been verified by considering three test cases. In first non-ideal thermodynamics nozzle case, results from SU2-COOL agree well with results from other NICFD solvers and experiment data, with maximum difference less than 5% under viscous/inviscid ideal/non-ideal conditions. In second non-ideal gasdynamics nozzle case, results from SU2-COOL and NIMOC-CoolProp are identical. The density obtained from SU2-COOL and SU2-PR differ, and the difference increases with decreasing Z_l or increasing flow non-ideality, which shows the advantage of SU2-COOL under highly non-ideal conditions. In third non-classical rarefaction oblique shock case, results from SU2-PVdW differ from those from SU2-PR and SU2-COOL. Generally, PVdW model lose accuracy under highly non-ideal conditions. As reported in [25], the value of Γ computed from PR is smaller than that from multiparameter equation of state near critical point. Therefore, it is possible that under a certain working condition, Γ computed from SU2-PR is negative, opening the possibility of non-classical rarefaction shock; while Γ computed from SU2-COOL is positive and only classical compression shock can occur. Overall, it is necessary to use SU2-COOL for highly non-ideal flow to predict the flow field accurately.

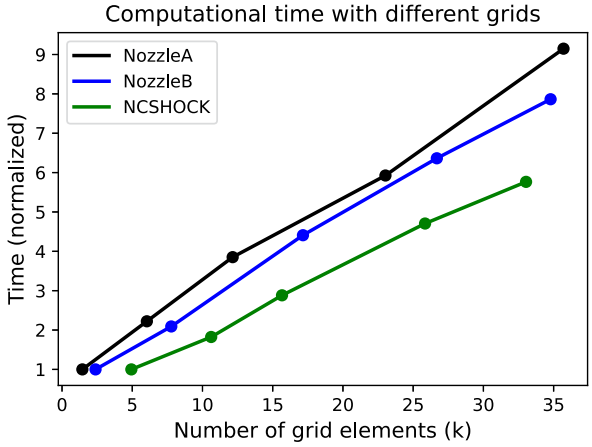

(a) Normalized computational time vs increasing number of grid elements.

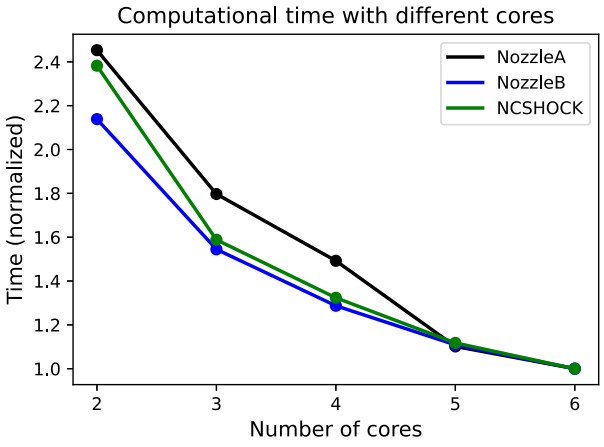

(b) Normalized computational time vs increasing number of CPU cores.

Fig. 19. Assessment of scalability with increasing workload and CPU cores with other numerical setup same. All simulations stop after 100 iterations.

Table 6
Computational time for simulations with different NICFD solver with same numerical setup. Time is normalized by the value related to SU2-PVdW in each test case. All simulations stop after 100 steps.

Solver	Nozzle A	Nozzle B	NCSHOCK
SU2-PVdW	1	1	1
SU2-PR	1.04	1.13	0.90
SU2-COOL	5.51	5.11	4.45
SU2-FluidProp	6.10	5.80	5.61

4.4. Computation efficiency

To assess the computational efficiency of SU2-COOL, the computational time is compared with other NICFD solver for three test cases with same numerical setup.

The results are summarized in Table 6. The computational time required by SU2-COOL is around five times longer than that by SU2-PVdW and SU2-PR. It is not surprising since at each iteration, SU2-COOL need call the external CoolProp library which implements the highly accurate but much more complex HEOS. Time spent by SU2-COOL and SU2-FluidProp is about the same since both of them call external thermophysical library.

5. Conclusion

The SU2-COOL solver, a fully open-source CFD framework for the numerical simulation of Non-Ideal Compressible Fluid Dynamics (NICFD) flows, is developed and verified. The framework interfaces two open-source software, namely, the CFD toolkit SU2 and the thermophysical library CoolProp. Two reference nozzle flow test cases are employed to verify the implementation, considering diverse fluids, thermodynamic models, and operating conditions. A non-classical centered Prandtl-Meyer expansion shock is also presented. The solution is verified against reference data from established solvers and validated against available measurements. Performance of SU2-COOL is also assessed.

The SU2-COOL framework is freely available from the `master` branch in the `SU2` GitHub repository [17]. The case files and data related to all test cases reported in this work can be obtained from [26]. Thanks to the integration with the CoolProp library, the software extends the current SU2 NICFD solver, which relies on a limited, embedded thermophysical library for NICFD computations, to an open-source thermodynamics library implementing very accurate technical and reference equations of state for pure fluids and mixtures.

CRediT authorship contribution statement

Peng Yan: Writing – original draft, Visualization, Validation, Software, Methodology, Investigation, Formal analysis, Data curation. **Giulio Gori:** Writing – review & editing, Supervision, Software, Methodology, Conceptualization. **Marta Zocca:** Writing – review & editing, Validation, Supervision, Methodology, Investigation, Formal analysis, Conceptualization. **Alberto Guardone:** Writing – review & editing, Supervision, Project administration, Methodology, Investigation, Funding acquisition, Formal analysis, Conceptualization.

Declaration of competing interest

The authors declare the following financial interests/personal relationships which may be considered as potential competing interests: Peng Yan reports financial support was provided by China Scholarship Council, scholarship No. 202106020057. If there are other authors, they declare that they have no known competing financial interests or personal relationships that could have appeared to influence the work reported in this paper.

Acknowledgements

This research is partly supported by China Scholarship Council, scholarship No. 202106020057, Project CSC-POLIMI PhD.

Data availability

A link to the data in GitHub is given in the paper.

References

[1] Alberto Guardone, Piero Colonna, Matteo Pini, Andrea Spinelli, Nonideal compressible fluid dynamics of dense vapors and supercritical fluids, Annu. Rev. Fluid Mech. 56 (2024) 241–269, https://doi.org/10.1146/annurev-fluid-120720-033342.
[2] Ennio Macchi, Marco Astolfi, Organic Rankine Cycle (ORC) Power Systems: Technologies and Applications, Woodhead Publishing, 2016.
[3] C. Zamfirescu, I. Dincer, Performance investigation of high-temperature heat pumps with various bzt working fluids, Thermochim. Acta 488 (1–2) (2009) 66–77, https://doi.org/10.1016/j.tca.2009.01.028.
[4] Martin T. White, Giuseppe Bianchi, Lei Chai, Savvas A. Tassou, Abdulnaser I. Sayma, Review of supercritical co2 technologies and systems for power generation, Appl. Therm. Eng. 185 (2021) 116447, https://doi.org/10.1016/j.applthermaleng.2020.116447.
[5] Pablo G. Debenedetti, Jean W. Tom, Xianmin Kwauk, S-D. Yeo, Rapid expansion of supercritical solutions (ress): fundamentals and applications, Fluid Phase Equilib. 82 (1993) 311–321, https://doi.org/10.1016/0378-3812(93)87155-T.
[6] Philip A. Thompson, A fundamental derivative in gasdynamics, Phys. Fluids 14 (9) (1971) 1843–1849, https://doi.org/10.1063/1.1693693.

[7] Salvatore Vitale, Giulio Gori, Matteo Pini, Alberto Guardone, Thomas D. Economon, Francisco Palacios, Juan J. Alonso, Piero Colonna, Extension of the su2 open source cfd code to the simulation of turbulent flows of fuids modelled with complex thermophysical laws, in: 22nd AIAA Computational Fluid Dynamics Conference, 2015, p. 2760.
[8] Jianhui Qi, Jinliang Xu, Kuihua Han, Ingo HJ Jahn, Development and validation of a Riemann solver in openfoam® for non-ideal compressible fluid dynamics, Eng. Appl. Comput. Fluid Mech. 16 (1) (2022) 116–140, https://doi.org/10.1080/19942060.2021.2002723.
[9] Ettore Fadiga, Nicola Casari, Alessio Suman, Michele Pinelli, Coolfoam: the coolprop wrapper for openfoam, Comput. Phys. Commun. 250 (2020) 107047, https://doi.org/10.1016/j.cpc.2019.107047.
[10] Alessandro Romei, Davide Vimercati, Giacomo Persico, Alberto Guardone, Non-ideal compressible flows in supersonic turbine cascades, J. Fluid Mech. 882 (2020) A12, https://doi.org/10.1017/jfm.2019.796.
[11] Giulio Gori, P. Molesini, G. Persico, Alberto Guardone, Non-ideal compressible-fluid dynamics of fast-response pressure probes for unsteady flow measurements in turbomachinery, J. Phys. Conf. Ser. 821 (2017) 012005, https://doi.org/10.1088/1742-6596/821/1/012005.
[12] Giulio Gori, Marta Zocca, Giorgia Cammi, Andrea Spinelli, Pietro Marco Congedo, Alberto Guardone, Accuracy assessment of the non-ideal computational fluid dynamics model for siloxane mdm from the open-source su2 suite, Eur. J. Mech. B, Fluids 79 (2020) 109–120, https://doi.org/10.1016/j.euromechflu.2019.08.014.
[13] Eric W. Lemmon, Marcia L. Huber, Mark O. McLinden, et al., Nist standard reference database 23. Reference fluid thermodynamic and transport properties (REFPROP), version, 9, 2010.
[14] Piero Colonna, T.P. Van der Stelt, Fluidprop: a program for the estimation of thermo physical properties of fluids, Energy Technology Section, Delft University of Technology, The Netherlands, 2004.
[15] Ian H. Bell, Jorrit Wronski, Sylvain Quoilin, Vincent Lemort, Pure and pseudo-pure fluid thermophysical property evaluation and the open-source thermophysical property library coolprop, Ind. Eng. Chem. Res. 53 (6) (2014) 2498–2508, https://doi.org/10.1021/ie4033999.
[16] Thomas D. Economon, Francisco Palacios, Sean R. Copeland, Trent W. Lukaczyk, Juan J. Alonso, Su2: an open-source suite for multiphysics simulation and design, AIAA J. 54 (3) (2016) 828–846, https://doi.org/10.2514/1.J053813.
[17] SU2 code developers. Master branch, https://github.com/su2code/SU2.git, 2023.
[18] Andrea Spinelli, Giorgia Cammi, Simone Gallarini, Marta Zocca, Fabio Cozzi, Paolo Gaetani, Vincenzo Dossena, Alberto Guardone, Experimental evidence of non-ideal compressible effects in expanding flow of a high molecular complexity vapor, Exp. Fluids 59 (2018) 1–16, https://doi.org/10.1007/s00348-018-2578-0.
[19] Christophe Geuzaine, Jean-François Remacle, Gmsh: a 3-d finite element mesh generator with built-in pre- and post-processing facilities, Int. J. Numer. Methods Eng. 79 (11) (2009) 1309–1331, https://doi.org/10.1002/nme.2579.
[20] Florianr Menter, Zonal two equation kw turbulence models for aerodynamic flows, in: 23rd Fluid Dynamics, Plasmadynamics, and Lasers Conference, 1993, p. 2906.
[21] Matteo Pini, S. Vitale, Piero Colonna, Giulio Gori, Alberto Guardone, T. Economon, J.J. Alonso, F. Palacios, Su2: the open-source software for non-ideal compressible flows, J. Phys. Conf. Ser. 821 (2017) 012013, https://doi.org/10.1088/1742-6596/821/1/012013.
[22] Marta Zocca, Paolo Gajoni, Alberto Guardone, Nimoc: a design and analysis tool for supersonic nozzles under non-ideal compressible flow conditions, J. Comput. Appl. Math. 429 (2023) 115210, https://doi.org/10.1016/j.cam.2023.115210.
[23] M.S. Cramer, LM Best Steady, Isentropic flows of dense gases, Phys. Fluids A, Fluid Dyn. 3 (1) (1991) 219–226, https://doi.org/10.1063/1.857855.
[24] Peng Yan, Camilla Cecilia Conti, Giulio Gori, Barbara Re, Alberto Guardone, Numerical simulation of ideal and non-ideal under-expanded supersonic jets with adaptive grids, J. Comput. Appl. Math. 427 (2023) 115169, https://doi.org/10.1016/j.cam.2023.115169.
[25] P. Colonna, N.R. Nannan, Alberto Guardone, T.P. Van der Stelt, On the computation of the fundamental derivative of gas dynamics using equations of state, Fluid Phase Equilib. 286 (1) (2009) 43–54, https://doi.org/10.1016/j.fluid.2009.07.021.
[26] Peng Yan, Original files and data of testcases, https://github.com/PENGYAN777/coolprop.git, 2023.